

HERMES Radio

Energy and Spectral Efficient Transmitter architectures for small satellites

Karunanithi, Visweswaran; Verhoeven, C.J.M. (Chris); Vaucher, Cicero S.

DOI

[10.1109/AERO53065.2022.9843200](https://doi.org/10.1109/AERO53065.2022.9843200)

Publication date

2022

Document Version

Final published version

Published in

Proceedings of the 2022 IEEE Aerospace Conference (AERO)

Citation (APA)

Karunanithi, V., Verhoeven, C. J. M., & Vaucher, C. S. (2022). HERMES Radio: Energy and Spectral Efficient Transmitter architectures for small satellites. In *Proceedings of the 2022 IEEE Aerospace Conference (AERO)* (pp. 1-10). Article 9843200 (IEEE Aerospace Conference Proceedings; Vol. 2022-March). IEEE. <https://doi.org/10.1109/AERO53065.2022.9843200>

Important note

To cite this publication, please use the final published version (if applicable).
Please check the document version above.

Copyright

Other than for strictly personal use, it is not permitted to download, forward or distribute the text or part of it, without the consent of the author(s) and/or copyright holder(s), unless the work is under an open content license such as Creative Commons.

Takedown policy

Please contact us and provide details if you believe this document breaches copyrights.
We will remove access to the work immediately and investigate your claim.

Green Open Access added to TU Delft Institutional Repository

'You share, we take care!' - Taverne project

<https://www.openaccess.nl/en/you-share-we-take-care>

Otherwise as indicated in the copyright section: the publisher is the copyright holder of this work and the author uses the Dutch legislation to make this work public.

HERMES Radio: Energy and Spectral Efficient Transmitter architectures for small satellites

Visweswaran Karunanithi ^{a,b}, C.J.M (Chris) Verhoeven ^a, Cicero S. Vaucher ^{a,c}

^a Delft University of Technology, The Netherlands

Mekelweg 5, 2628 CD Delft, The Netherlands

V.Karunanithi-1@tudelft.nl

^b Innovative Solutions In Space B.V, The Netherlands

^c NXP Semiconductors, The Netherlands

Abstract: As the complexity of nanosatellite missions have increased over time, the data generated on-board nanosatellites have increased multiple folds. As a result, there is a need to downlink large amounts of data. Multiple nanosatellite missions have started using spectral efficient modulation schemes recommended in DVB.S2 and DVB.S2X to make the best use of the available spectrum. One of the main challenges in adopting higher order modulation schemes is to power-efficiently upconvert and amplify the baseband signals. All the lost efficiency in converting the DC power to the RF output is dissipated as heat and the relatively small thermal mass of nanosatellites poses thermal management challenges.

As a first step to addressing the challenge of improving the power efficiency of the communication module, optimization techniques to improve the Peak to Average Power Ratio (PAPR) of the modulation schemes (16/32-APSK) are discussed in this paper. The PAPR of 16-APSK reduces by ~2 dB by incorporating filtering techniques discussed in this paper. Further, a well-known efficiency and linearity enhancement technique; Out-phasing/LINC (Linear Amplification using Non-linear Components) is discussed. As a variant of the out-phasing architecture, a novel approach is proposed using two circularly polarized antenna to transmit the constant envelope signals in opposite polarizations and signal combining is performed at the receiver. Simulations results are used to demonstrate how higher efficiencies can be achieved using the proposed architecture.

TABLE OF CONTENT

1. INTRODUCTION	1
2. MODULATION SCHEMES.....	2
3. EFFICIENCY AND LINEARITY ENHANCEMENT TECHNIQUES	3
4. PROPOSED TRANSMITTER ARCHITECTURE.	4
5. DUAL POLARIZED ANTENNA DESIGN	7
6. SUMMARY	8
7. AKNOWLEGMENT	9

1. INTRODUCTION

Nanosatellite missions are undergoing a paradigm shift in its complexity and as a result need high data-rate radios to

transmit their payload data to the ground stations or in some case exchange large volumes of data between nanosatellites[1]. This has resulted in the need to develop high data-rate radios that are both energy and spectral efficient. In the past, nanosatellite missions made use of low data-rate radios, on the order of 1.2 to 9.6 kbps to communicate with their ground stations. This trend has gradually changed and nanosatellite missions in recent time have crossed the 1Gbps downlink data-rates. A good example of such mission is the Planet's High-Speed Downlink 2 (HSD2) radios that achieved 1.6 Gbps downlink on a 3U nanosatellite mission [2]. Although this radio achieved a high data-rates, the potential drawback of such systems is the heat dissipated by them; in-order to achieve a 2-Watts RF transmit power, the DC power consumption of the system is ~50 Watts. This means ~48 Watts is dissipated as heat and for the small volume of nanosatellites, dissipating this heat can be a challenge. In order to achieve high data-rates in the available signal bandwidths, spectral efficient modulation schemes such as 16/32/64-APSK modulation schemes are adopted, which is one of the main reasons of degradation in the system efficiency. Apart from the processing power needed in the baseband, the high Peak to Average Ratio (PAPR) inherent in these modulation schemes result in degradation of the Power Added Efficiency (PAE) of the transmitter [3].

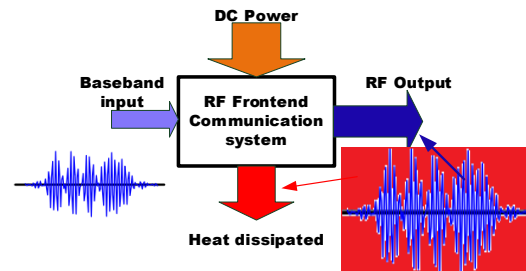


Figure 1. Primary contributor of heat dissipation in the RF-frontend of a communication system.

The Figure-1 depicts the primary contributor of heat dissipation in the RF-frontend of a communication system.

Although, the amplitude variation in the signal helps improving the spectral efficiency of the signal, it has an impact on the power efficiency of the system.

In-order to achieve good spectral and energy efficiency, linearization and efficiency enhancement techniques need to be incorporated in the transmitters [3]. Some of the well-known techniques include Out-phasing transmitters, also commonly known as LINC transmitters, Doherty transmitter, Envelope tracking transmitters, etc. From the literature, it was found that efficiency and linearity enhancement techniques are not very commonly used in nanosatellites. This could be primarily because, the use of spectral efficient modulation schemes in nanosatellite missions is very recent and implementation of efficiency and linearity enhancement techniques involves an implementation complexity and is not a commercially off-the-shelf approach.

In this paper, a simple implementation of out-phasing transmitter using two circularly polarized antennas is discussed. The preliminary research conducted in [4], where out-phasing/LINC transmitter was implemented for APSK modulation schemes show a very good improvement in performance, it was also proposed in the future works that a cross-dipole fed through a 90 degrees hybrid (Turnstile antenna) could be an option to transmit the two constant envelope signals $S_1(t)$ and $S_2(t)$ on two different polarizations.

This paper is organized as follows: Section 2 discusses some of the techniques to improve the PAPR of existing modulation schemes using 16-APSK as an example. Section-3 introduces out-phasing transmitter architecture from literature, some of the commonly used power combining techniques. The proposed transmitter architecture to improve PAE is discussed in Section 4. The antenna design and its performance in the context of the proposed architecture is discussed in Section-5, Inferences made out of the simulations are discussed in Section-6 and the conclusions are presented in Section-7.

2. MODULATION SCHEMES

One of the methods to improve the PAE of the RF-frontend is by minimizing the PAPR of the transmitted constellation. The PAPR of the standard modulation schemes recommended in DVB-S2 and S2X can be improved by polar filtering, this is widely discussed in [1]. One of the main drawbacks of polar filtering is the bandwidth expansion. This technique could still be of interest at mmWave frequencies as large bandwidths are available and large PAPR at mmWave frequencies can have a larger impact on the PAE of the front-end. Apart from polar filtering, another approach discussed here is to optimize the radius ratio of the constellations to improve the PAPR and then applying polar filtering helps improving the PAPR further. A comparison of the radius ratios of 1.75, 2 and 3 for 16-APSK is performed to determine the improvement in PAPR. Figure 2 shows a comparison between normal 16-APSK and polar filtered 16-APSK for a radius ratio of 1.75.

In both cases, the individual bits are SRRC filtered with a roll-off of 0.35.

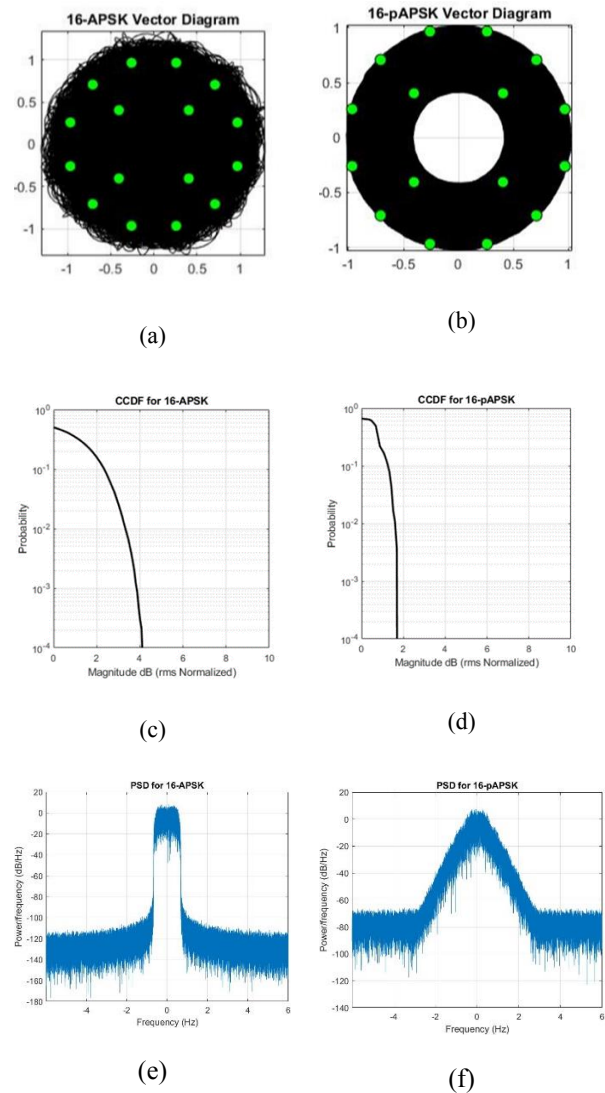


Figure 2. 16-APSK with a radius ratio of 1.75, (a) Normal 16-APSK, (b) Filtered 16-APSK, (c) CCDF for unfiltered 16-APSK, (d) CCDF for filtered, (e) PSD of 16-APSK, (f) PSD of Filtered 16-APSK.

The Table 1 summarizes the CCDF (Complementary Cumulative Distribution Function) of normal and polar filtered 16-APSK for various radius ratios. The CCDF is another representation of the PAPR seen by the TX-frontend.

Table 1 CCDF of unfiltered and polar filtered 16-APSK

Radius Ratios	CCDF of Normal 16-APSK [dB]	CCDF of Polar Filtered 16-APSK
1.75	4 dB	1.8 dB

2	4.1 dB	2 dB
3	4.2 dB	2.5 dB

The change in radius ratio translates to moving the constellation symbols either close to each other or away, which can lead to a change in the required E_b/N_0 (Energy per bit to noise spectral density ratio) needed to receive a symbol correctly.

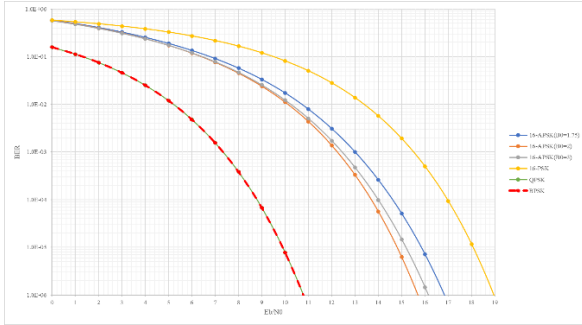


Figure 3 E_b/N_0 of 16-APSK for various radius ratios in relation to QPSK and 16-PSK.

Figure 3 shows the E_b/N_0 of 16-APSK for various radius ratios in relation to QPSK and 16-PSK. This is calculated based on the Euclidean distance between the symbols in the constellation. It can be seen that, although the radius ratio of 1.75 provides the best CCDF, the closer proximity between the symbols in the inner and outer ring increases the required E_b/N_0 by 1 dB at a BER of 10^{-5} . An optimal radius ratio of 2 provides the lowest E_b/N_0 with the best CCDF of 4.1 dB for normal 16-APSK and 2 dB for polar filtered 16-APSK. Hence, adopting polar filtering and optimizing the radius ratio for CCDF and E_b/N_0 , helps in achieving lower PAPR and results in lower heat dissipation, provided the bandwidth expansion is acceptable. The subsequent section discusses transmitter architectures that can further help improve the energy efficiency of the RF-frontend.

3. EFFICIENCY AND LINEARITY ENHANCEMENT TECHNIQUES

A classic out-phasing transmitter or also known as LINC transmitter uses the technique of converting an amplitude and phase modulated signal such as APSK into two constant envelope signals and amplifying them separately using efficient amplifiers classes such as Class-D, E, F etc and combining the amplified signals before radiating it through an antenna. The working principle of an out-phasing amplifier is shown in the Figure 4.

The complex amplitude and phase modulated signal $S(t)$ is split into $S_1(t)$ and $S_2(t)$, these individual paths are amplified

to $G \cdot S_1(t)$ and $G \cdot S_2(t)$. The two signal paths are then combined to obtain $G' \cdot S(t)$.

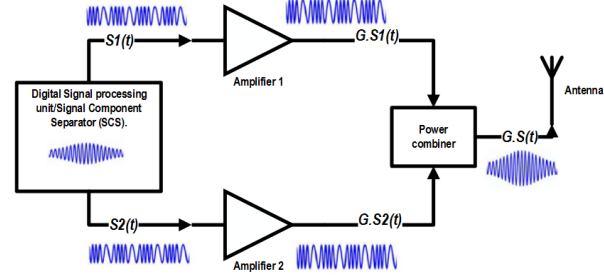


Figure 4. Conventional out-phasing transmitter

The function of a signal component separator (SCS) can be explained better using a constellation diagram as shown in Figure 5 below:

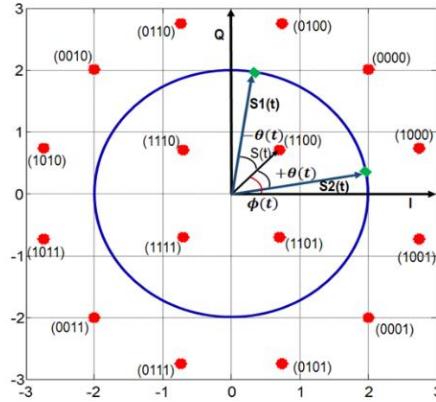


Figure 5. Function of SCS on 16-APSK constellation.

The $S(t)$ in Figure 5 can be represented as:

$$S(t) = r(t) \cdot e^{j(\omega t + \varphi(t))}$$

$r(t)$ is the time varying amplitude information and $\varphi(t)$ is the time varying phase information.

The time varying amplitude information can be represented as:

$$r(t) = r_{max} \cos(\theta(t))$$

Or,

$$r(t) = \frac{r_{max}}{2} (e^{j\theta(t)} + e^{-j\theta(t)})$$

Substituting for $r(t)$ in the equation for $S(t)$, we get:

$$S(t) = \frac{r_{max}}{2} (e^{j(\omega t + \varphi(t) + \theta(t))} + e^{j(\omega t + \varphi(t) - \theta(t))})$$

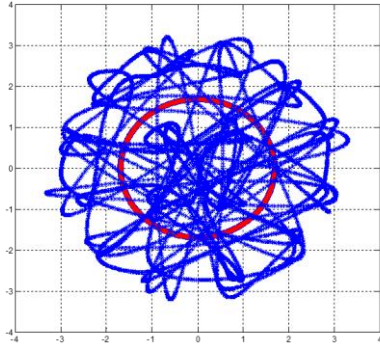


Figure 6. Vector plot of a 16-APSK signal (in blue) when passed through an SRRC filter and the corresponding constant envelope signal (in Red).[4]

This signal can now be split into two constant envelope signals as:

$$S(t) = S1(t) + S2(t)$$

Where:

$$S1(t) = \frac{r_{max}}{2} (e^{j(\omega t + \varphi(t) + \theta(t))})$$

$$S2(t) = \frac{r_{max}}{2} (e^{j(\omega t + \varphi(t) - \theta(t))})$$

As it can be seen from the above two equations, S(t) is split into two constant envelope signals S1(t) and S2(t) which are out of phase by $\pm \theta(t)$, which is known as the out-phasing angle. Hence, the transmitter is named out-phasing transmitter. The $\theta(t)$ can vary from 0 to $\pm 90^\circ$.

The primary factor that reduces the overall efficiency of an out-phasing transmitter is the power combiner stage, since the two constant envelope signals that are fed to the power combiner are not always in-phase, the efficiency of isolating power combiners drop at larger out-phasing angles [4][5][6][7]. In order to improve the efficiency of the combiner, Chireix combiners were introduced. The literature [3][8][9] elaborates the implementation of Chireix combiner.

A novel concept is addressed in this paper where the two constant envelope signals G.S1(t) and G.S2(t) are transmitted separately on two different polarizations (RHCP and LHCP) and the signals are combined at the receiver to reconstruct the original spectral-efficient, non-constant envelope signal. Some of the earlier implementations of antenna combiners in out-phasing transmitters are discussed in [10][11][12][13], unlike the earlier work, the proposed design does not spatially combine the signals. In an earlier research carried out by the author, such implementation was proposed for cubesats [3]. Here the two constant envelope signals were fed to a cross dipole through a 90 degrees hybrid, and it was observed that the out-phasing angles do not have an effect on the radiation pattern of the antenna in the end-fire direction. This concept was later demonstrated using dual fed linear polarized patch antenna in [14] and it was seen that the overall system efficiency improved. Although the proposed architecture in

this work uses two antennas, one for RHCP and one for LHCP, it is possible to use a single dual-circularly polarized antenna that has sufficient cross polar discrimination (XPD). The subsequent section elaborates the proposed transmitter architecture.

4. PROPOSED TRANSMITTER ARCHITECTURE

The proposed transmitter architecture is a modified Out-phasing/LINC architecture. A block diagram of the proposed transmitter architecture is shown in the Figure 7 below. The pulse-shaped IQ waveform is fed to a SCS where the waveform is split into two constant envelopes S1(t) and S2(t). The S1(t) and S2(t) are upconverted using quadrature mixers to the desired frequency and fed to two identical amplification paths. The outputs of the driver stage PAs are fed to highly efficient non-linear PAs, such as Class-C, D, E or F PAs. Since the constant envelope signals do not have amplitude variations, peak efficiencies are achieved in the RF-frontend.

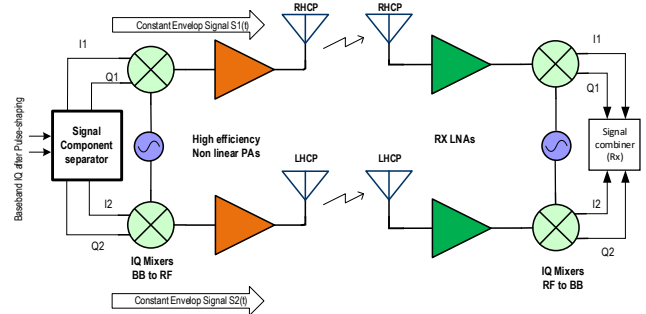


Figure 7. Proposed Tx/Rx architecture using polarization diversity.

One of the main drawbacks of LINC/Out-phasing transmitter architecture is, when the non-constant envelope signal is split into constant envelope signals, bandwidth expansion occurs in the individual signal paths. This can be seen in the output power spectrum of S(t), S1(t) and S2(t) shown in Figure 8.

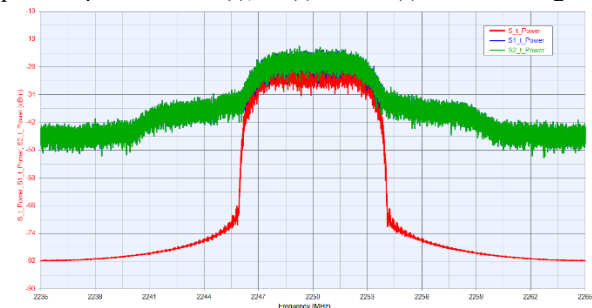


Figure 8. Output power spectrum of S(t) in red, S1(t) in blue and S2(t) in green.

The simulated output spectrum is 6Msps, 32-APSK at 2250MHz, and pulse shaped with SRRC filter (Roll-off = 0.35).

Although, this architecture helps in reducing the PAPR, the occupied bandwidth expands in the individual signal paths.

As a result of bandwidth expansion, this architecture is not suitable at lower frequencies such as UHF, S-band and X-band. At mmWave frequencies where large bandwidths are available, this approach helps in improving the PAE by lowering the PAPR at the cost of bandwidth.

Since the input to signal component separator (SCS) is an already pulse shaped IQ waveform and when this waveform gets split into constant envelope signals using the equations discussed in Section-3, the output waveforms are transformed into two constant amplitude waveforms and all the information is translated into the phase. This results in bandwidth expansion on the individual signal paths.

One of the methods to overcome bandwidth expansion and still use polarization diversity is to perform pulse shaping after the SCS. Instead of feeding the SCS with an already pulse shaped waveform, the pulse shaping is carried out on the output of SCS, namely $I_1(t)$, $Q_1(t)$, $I_2(t)$ and $Q_2(t)$. This architecture is depicted in the Figure 10. Now the pulse shaped waveforms are bandwidth limited and can be transmitted separately.

The simulated output power spectrum of $S(t)$, $S_1(t)$ and $S_2(t)$ is shown in Figure 9. The spectrum in red represents $S(t)$, blue represents $S_1(t)$ and red represents $S_2(t)$. The modulation scheme considered for this simulation is 32-APSK at a symbol rate of 6MSPs, the pulse shaping used is SRRC with a roll-off of 0.35.

The proposed architecture is called HERMES architecture, the abbreviation stands for High data-rate Energy and Spectral Efficient Radios for Small satellites. The proposed HERMES architecture was simulated in Simulink to validate the full chain, the Simulink model is shown in Figure 11. The non-pulse shaped IQ waveform is sent to a SCS block that separates the signal into two constant envelope signals $S_1(t)$ and $S_2(t)$. The signal component separation was implemented based on the algorithm proposed in [15].

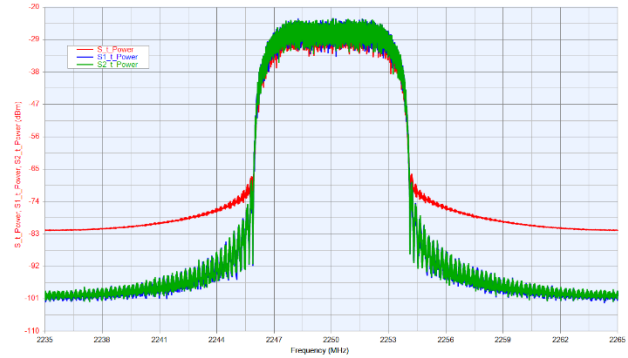


Figure 9. Output power spectrum of pulse shaped $S_1(t)$ and $S_2(t)$ in comparison with $S(t)$.

One of the drawbacks seen in HERMES architecture is that the pulse shaping done after SCS introduces a PAPR in the split waveforms $S_1(t)$ and $S_2(t)$. This PAPR is introduced only due to the pulse shaping filter. The table below shows the PAPR of various modulation schemes in comparison with the PAPR of $S_1(t)$ and $S_2(t)$.

Table 2. PAPR of various modulations schemes in comparison with $S_1(t)$ and $S_2(t)$.

Modulation scheme	PAPR of $S(t)$ (dB)	PAPR of $S_1(t)$ (dB)	PAPR of $S_2(t)$ (dB)
16-APSK	4.1	3.2	3.2
32-APSK	5	3.24	3.3
64-APSK	6.02	3.2	3.2
256-APSK	7.14	3.4	3.5

As can be seen in the table, the PAPR of $S_1(t)$ and $S_2(t)$ does not increase drastically as the spectral efficiency increases.

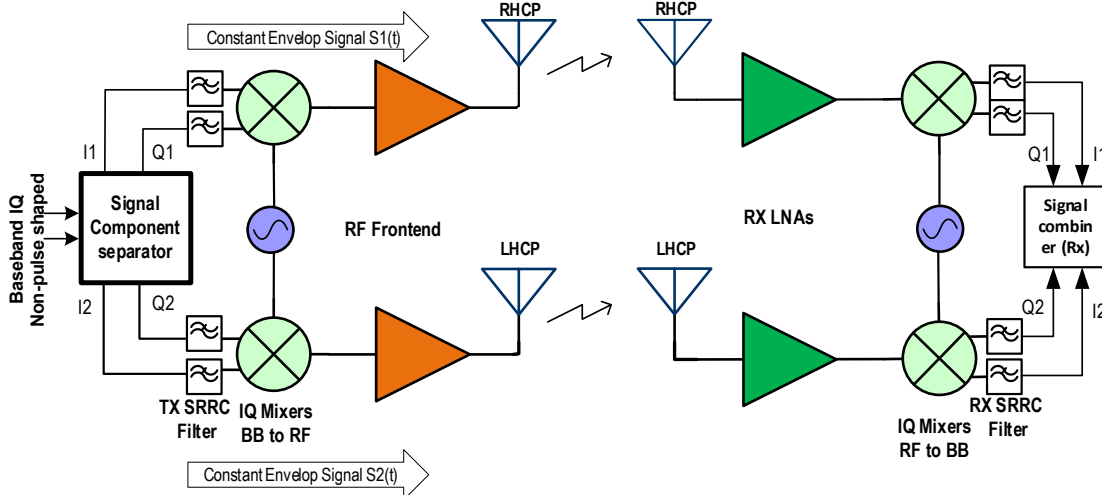


Figure 10. Proposed Tx/Rx architecture using polarization diversity with modified pulse shaping filters.

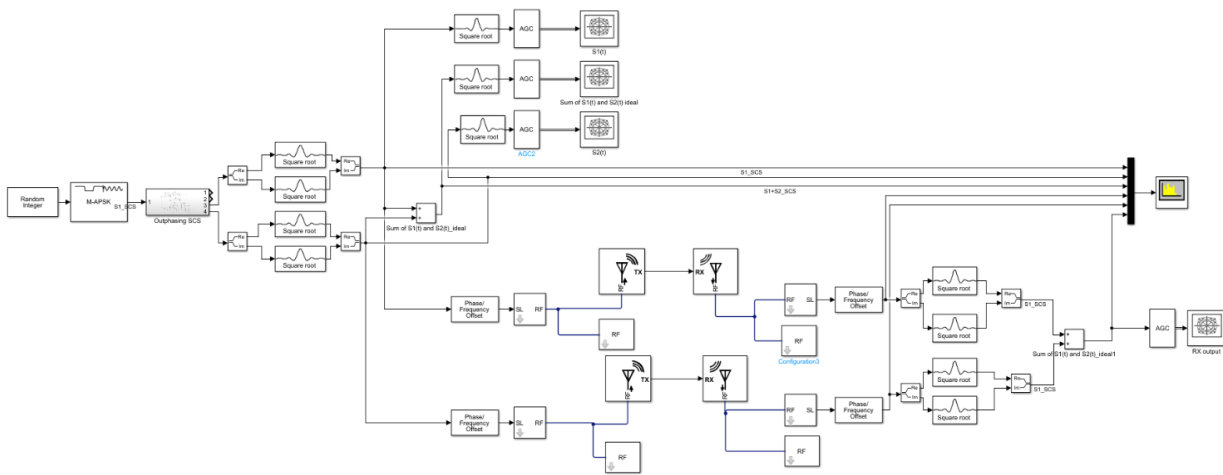


Figure 11. Simulink model to validate end-to-end of the proposed Tx/Rx architecture.

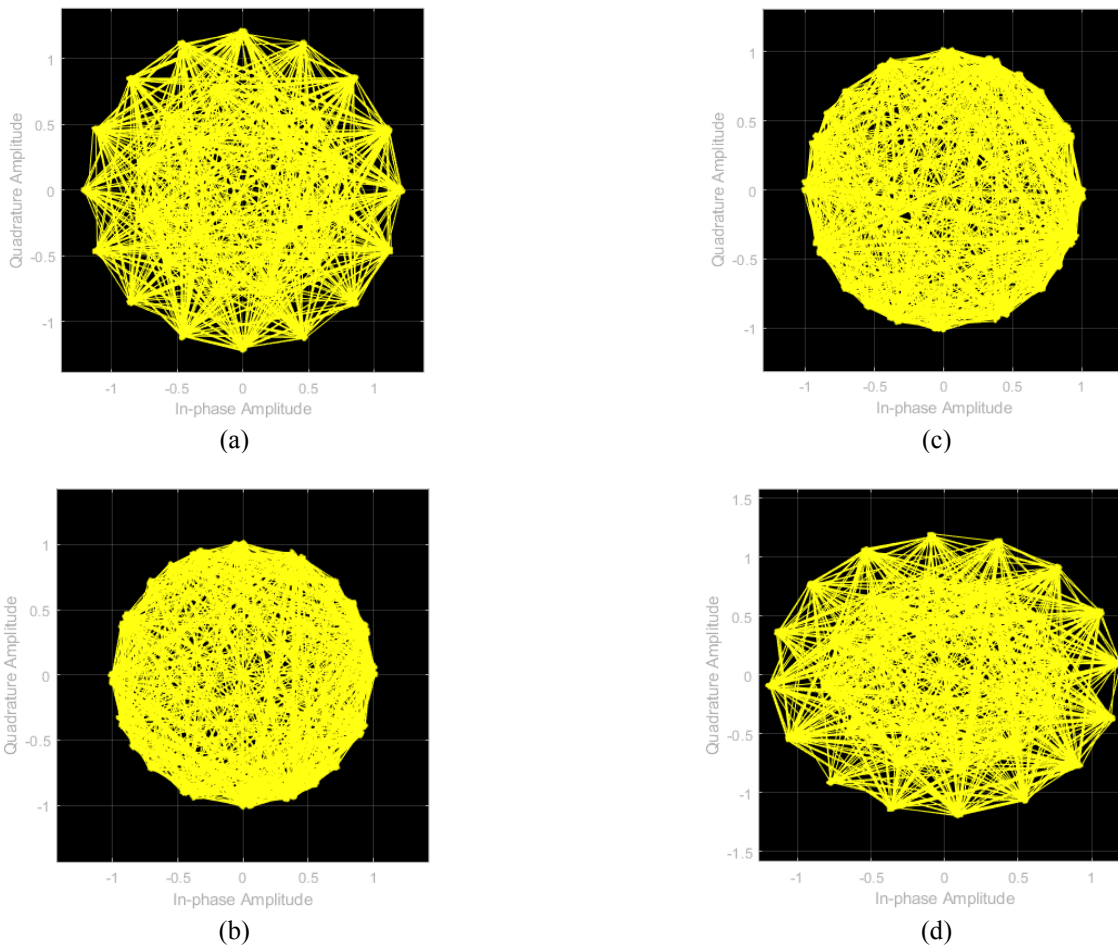


Figure 12. (a) IQ plot of un-filtered baseband input to SCS, (b) IQ plot of $S1(t)$, (c) IQ plot of filtered $S2(t)$, (d) IQ plot of received signal.

5. DUAL POLARIZED ANTENNA DESIGN

The use of polarization diversity has been demonstrated in satellite downlinks as discussed in [2], [16]. For the validation of the proposed HERMES architecture, two opposite circularly polarized patch antennas are designed at 2250 MHz. This frequency was chosen only for the ease of demonstration, the architecture can be scaled-up to higher frequencies as well. Another approach is to use a single dual circularly polarized antenna similar to the X-band choke ring horn antenna used in NASA's SWOT Mission [17]. For such antennas, the cross-pol discrimination (XPD) can play a very important role in determining the degradation in the performance. The XPD is defined as the ratio of co-pol power to the cross-pol converted leakage power. As explained in [18], in-order to achieve a cross-pol degradation of less than 1 dB, the XPD needs to be higher than 15dB.

The designed two circularly polarized patch antennas are shown in Figure 13, The individual antenna is a dual-fed circular patch antenna is fed through hybrid couplers, the feeding network for the two patches is shown in Figure 14. The unused port of the hybrid couplers is terminated using a 50 Ohms load.

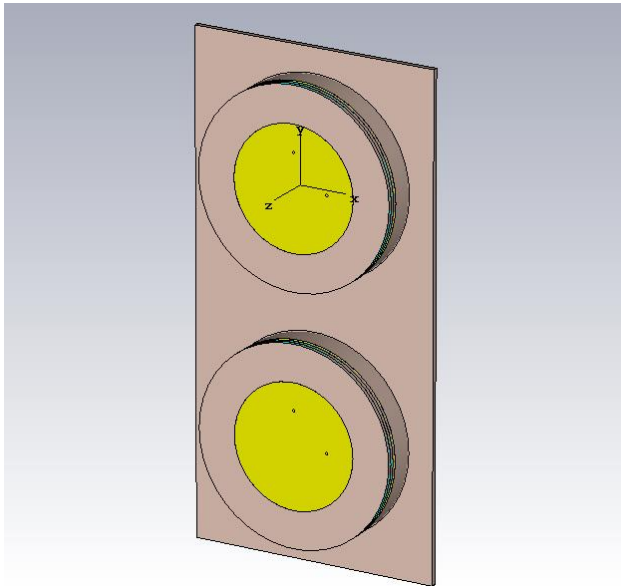


Figure 13. Two circularly polarized patch antennas.

In the feeding network, Port-1 corresponds to RHCP and Port-2 corresponds to LHCP. The S-parameters seen at the feeding network is shown in Figure 15. The S11 and S22 are below -15dB and more importantly, the isolation between Port-1 and Port-2 is less than -30 dB. This is important, because the two waveforms are separated by an out-phasing angle $\pm\theta(t)$ and when the two signals are separated by large out-phasing angles, the isolation helps in the RF-frontend see the same impedance (the reactance part does not change).

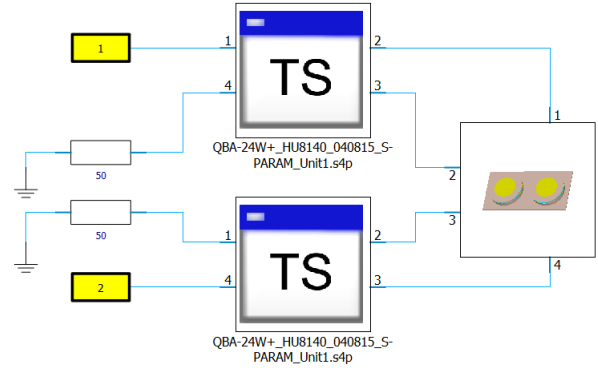


Figure 14. Antenna feeding network. Port-1 corresponds to RHCP, Port-2 corresponds to LHCP.

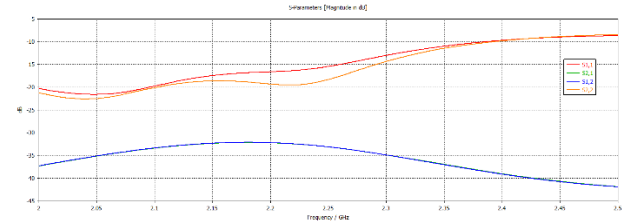


Figure 15. S-parameters as seen at the feeding network.

As the out-phasing angles change by $\pm\theta(t)$, it can have an impact on the radiation patterns of the two antennas, this is depicted in Figure 16 and Figure 17.

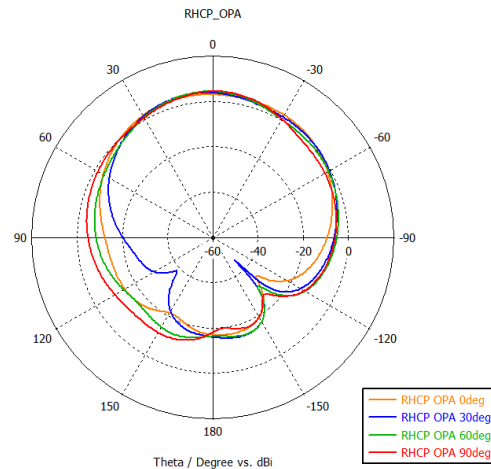


Figure 16. Radiation pattern of RHCP antenna for out-phasing angles: 0, 30, 60 and 90 deg.

6. SUMMARY

The adoption of spectral efficient modulation schemes in small satellite missions have become common, resulting in the need for power efficient RF-frontends. The large PAPR of spectral efficient modulation schemes pose a challenge on the RF frontend to amplify the signal with minimal distortion and at the same time achieve high PAE. Although linear PAs can amplify the signal with minimal distortion, the large PAPRs would result in large heat dissipation. Thus, small thermal mass of small satellites has resulted in investigating efficiency and linearity enhancement techniques to reduce the issue of heat dissipation. Although there are well known efficiency and linearity enhancement techniques, this paper addresses the possibility to improve the PAR of the RF-frontend by changing the radius ratio of the constellation points and performing polar filtering. The 16-APSK is used as an example and it was observed that although lower radius ratio results in lower PAPR, a radius ratio below 2 for 16-APSK worsens the E_b/N_0 . With polar filtering, although good PAPR is achieved, it comes at the price of bandwidth expansion. This might not be a bad option to consider at mmWave frequencies as large bandwidths are available.

The second part of this paper addresses radio architectures that can improve the PAE of the RF-frontend. A novel concept of polarization diversity was introduced in combination with modified LINC/Outphasing architecture. The proposed architecture is called HERMES. In this paper, the feasibility of HERMES architecture is validated using simulations and some of its implementation challenges were highlighted. Based on the simulation results, it was observed that this architecture suited better for higher order modulation schemes such as 64-APSK or 256-APSK compared to the lower order schemes such as QPSK, 16-APSK or 32-APSK. This is because the PAPR of the individual transmit paths remain between 3 to 3.5dB irrespective of the order of the modulation scheme and for higher order modulation scheme such as 256-APSK, which has a PAPR of 7.14 dB, the resultant PAPR is 3.5 dB in this individual transmit paths. This is ~ 3.5 dB improvement in the power back-off that the RF frontend has to handle. Since the performance of this system is highly dependent on line-of-sight communications, this architecture could be used for high data-rate space-to-earth links or Inter-satellite links.

One of the main components in implementing HERMES architecture is the dual circularly polarized antennas. In this paper, two opposite circularly polarized antennas were designed at S-band. The simulations validate that an XPD higher than 15 dB can be achieved using this configuration. This results in cross-pol degradation of less than 1dB. It was also validated that the change in out-phasing angles does not affect the gain along the end-fire direction, hence suitable to transmit two out of phase signals simultaneously. As the next steps this architecture will be tested in a lab with non-linear

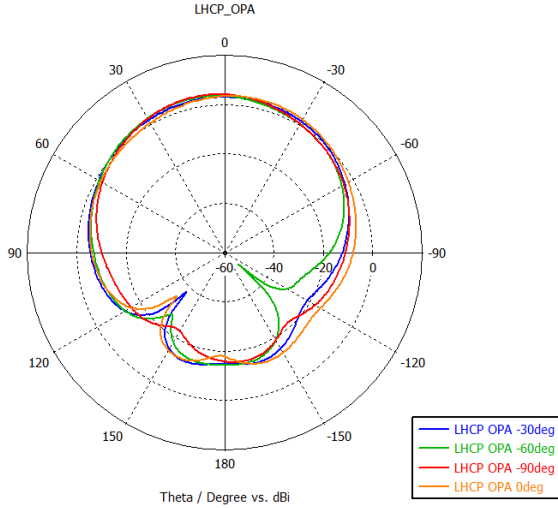


Figure 17. Radiation pattern of LHCP antenna for the out-phasing angles: 0, -30, -60, -90 deg.

It can be noticed in the radiation patterns, the change in out-phasing angles do not cause the gain to vary in the end-fire direction. This helps in using this two-antenna concept for the proposed transmitter architecture.

One other parameter that can have an influence on the performance of the system is the XPD of the two antennas. Figure 18 and Figure 19 show the XPD of the two antennas.

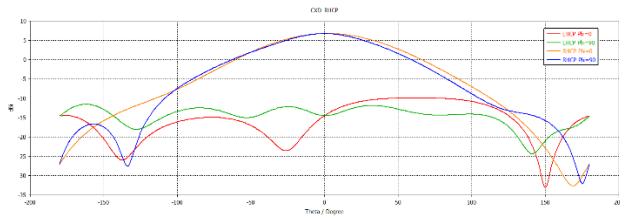


Figure 18. XPD of RHCP antenna at Phi = 0 and Phi = 90 deg.

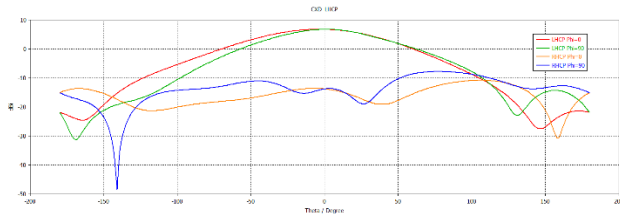


Figure 19. XPD of LHCP antenna at Phi=0 and Phi=90 deg.

As can be seen from the plots, the XPD of both the antennas are ~ 19 dB which is better than the expected 15dB, this results in a cross-pol degradation of less than 1dB[18].

components such as RF-PAs to better determine the system level performance.

7. AKNOWLEDGMENT

The authors thank the TKI funding, Netherlands and TU Delft for funding this work. The authors thank the industry partners Hyperion B.V and Innovative Solutions In Space B.V for extending their support and guidance.

8. REFERENCES

- [1] I. V. Karunanithi, C. J. M. Verhoeven, and E. W. McCune, 'Solutions to Data Congestion in Space; mmWave Communication for Nano-Satellites', in *2019 IEEE Aerospace Conference*, Mar. 2019, pp. 1–12, doi: 10.1109/AERO.2019.8742131.
- [2] K. Devaraj *et al.*, 'Planet High Speed Radio: Crossing Gbps from a 3U CubeSat', *33rd Annual AIAA/USU Conference on Small Satellites*. pp. 1–10, 2019, [Online]. Available: <https://digitalcommons.usu.edu/smallsat/2019/all2019/106>.
- [3] I. V. Karunanithi and C. J. M. Verhoeven, 'High Efficiency Transmitter Architecture for Nano-satellites'. 2014, [Online]. Available: <https://tudelft.on.worldcat.org/oclc/1008810957>.
- [4] V. Karunanithi, C. J. . C. Verhoeven, and W. Lubbers, 'LINC transmitter architecture for nano-satellite applications', in *2015 IEEE Aerospace Conference*, Mar. 2015, pp. 1–9, doi: 10.1109/AERO.2015.7119190.
- [5] D. Zhao and P. Reynaert, 'CMOS 60-GHz and E-band Power Amplifiers and Transmitters', *Springer*. 2015.
- [6] R. Montesinos, C. Berland, M. A. Hussein, O. Venard, and P. Descamps, 'Comparative analysis of LINC transmitter performances with class AB and class F power amplifiers', *2011 IEEE 9th International New Circuits and Systems Conference, NEWCAS 2011*. pp. 233–236, 2011, doi: 10.1109/NEWCAS.2011.5981298.
- [7] G. Poitau, A. Birafane, and A. Kouki, 'Experimental characterization of LINC outphasing combiners' efficiency and linearity', *Proceedings - 2004 IEEE Radio and Wireless Conference, RAWCON*. pp. 87–90, 2004, doi: 10.1109/rawcon.2004.1389078.
- [8] D. Cox, 'Linear Amplification with Nonlinear Components', *IEEE Trans. Commun.*, vol. 22, no. 12, pp. 1942–1945, Dec. 1974, doi: 10.1109/TCOM.1974.1092141.
- [9] F. Raab, 'Efficiency of Outphasing RF Power-Amplifier Systems', *IEEE Trans. Commun.*, vol. 33, no. 10, pp. 1094–1099, Oct. 1985, doi: 10.1109/TCOM.1985.1096219.
- [10] S. Gao and P. Gardner, 'Integrated antenna/power combiner for LINC radio transmitters', *IEEE Trans. Microw. Theory Tech.*, vol. 53, no. 3 II, pp. 1083–1088, 2005, doi: 10.1109/TMTT.2005.843491.
- [11] Y. Zhou, M. Y. W. Chia, X. Qing, and J. Yuan, 'RF spatial modulation using antenna arrays', *IEEE Trans. Antennas Propag.*, vol. 61, no. 10, pp. 5229–5236, 2013, doi: 10.1109/TAP.2013.2272596.
- [12] C. Liang and B. Razavi, 'Transmitter linearization by beamforming', *IEEE J. Solid-State Circuits*, vol. 46, no. 9, pp. 1956–1969, 2011, doi: 10.1109/JSSC.2011.2148530.
- [13] E. J. Martinez-Perez, F. Jalili, M. Shen, J. H. Mikkelsen, O. K. Jensen, and G. F. Pedersen, 'T-LINC Architecture with Digital Combination and Mismatch Correction in the Receiver', in *2019 IEEE Nordic Circuits and Systems Conference (NORCAS): NORCHIP and International Symposium of System-on-Chip (SoC)*, Oct. 2019, pp. 1–5, doi: 10.1109/NORCHIP.2019.8906983.
- [14] D. Tresnawan, P. F. M. Smulders, B. van Ark, and A. B. Smolders, 'Linear LINC transmitters using Dual-polarized Power-Combining Antennas', in *12th European Conference on Antennas and Propagation (EuCAP 2018)*, 2018, pp. 805 (4 pp.)–805 (4 pp.), doi: 10.1049/cp.2018.1164.
- [15] S. A. Hetzel, A. Bateman, and J. P. McGeehan, 'A LINC transmitter', in *[1991 Proceedings] 41st IEEE Vehicular Technology Conference*, pp. 133–137, doi: 10.1109/VETEC.1991.140461.
- [16] T. Kaneko, 'Dual Circularly Polarization X band 2Gbps Downlink Communication System of Earth Observation Satellite', 2018, [Online]. Available: <https://digitalcommons.usu.edu/smallsat/2018/all2018/325>.
- [17] N. Chahat, L. R. Amaro, J. Harrell, C. Wang, P. Estabrook, and S. A. Butman, 'X-Band Choke Ring Horn Telecom Antenna for Interference Mitigation on NASA's SWOT Mission', *IEEE Trans. Antennas Propag.*, vol. 64, no. 6, pp. 2075–2082, 2016, doi: 10.1109/TAP.2016.2546298.
- [18] E. Satorius, T. Jedrey, and C. Wang, *Impact of Cross-Polarization Interference on Dual Polarization Communication Systems*. 2018, pp. 1–23.

9. BIOGRAPHY



Ir. Visweswaran Karunanithi, is a PhD researcher at the Technical University of Delft. He is also an RF Systems Engineer at Innovative Solutions In Space B.V, Delft, Netherlands. His journey in the small-satellite industry started in 2008 when he started working on India's first student made Pico-satellite mission "STUDSAT-

1" as a communications system engineer. This was a part of his undergraduate project during his study at Nitte Meenakshi Institute of Technology, Bangalore, India, where he received his Bachelor degree (Electronics and Communications Engineering) in the year 2009. The satellite was launched in 2010. He then moved to the Netherlands to join Innovative Solutions In Space B.V in 2011 starting his career as Jr.RF and Ground systems engineer. Alongside his work, he received his Masters degree from Technical University of Delft from the department of Microelectronics with a specialization in RF and antenna design. After completing his Masters, he continued to work at Innovative Solutions In Space B.V as RF Systems Engineer and Business Developer till 2017. In 2017 he started as PhD researcher at TU Delft. His areas of interests are Small satellites, RF front-end design, High efficiency PA design, Antenna design and EMC testing.



Ir. Dr. C.J.M. (Chris) Verhoeven is an associate professor in the Department of Microelectronics at the Delft University of Technology since 1999. His research interests are systematic analog design, RF circuits, adaptive radio systems, sensor electronics and avionics for

drones, sounding rockets and nano-satellites. From 2007-2018 he was part-time working at the Faculty of Aerospace Engineering at the Space Systems Engineering lab. He was responsible for the design and implementation of electronics for the Delfi-C3 nano-satellite which was launched in 2008 and that is still operational after nearly ten years. He is still involved in the development of future nano-satellite missions of the TU Delft and one of the initiators of the national project OLFAR (Orbiting Low Frequency Array); a radio telescope based on a swarm of nano-satellites in moon orbit.

Since 2013 Chris Verhoeven, together with Guido de Croon, leads the Swarm theme of the **TU Delft Robotics**

Institute, which conducts research in the field of swarms of underwater robots, autonomous drones and rovers and nano-satellites and supports student research into controlled sounding rockets in the Korolev Lab of the Institute. Along with Andre Schiele he leads the **Space Robotics Theme** of the **TU Delft Space Institute**, with a focus on micro-propulsion and aerospace mechatronics.



Prof. Dr. Cicero S. Vaucher was born in Sao Francisco de Assis, Brazil, in 1968. He received the Ph.D. degree in Electrical Engineering from the University of Twente in 2001. He joined the Philips Natuurkundige Laboratorium in 1990 and worked in the

Integrated Transceivers group until 2006. He then joined NXP Semiconductors, when Philips Semiconductors became an independent company. He is presently with the Infotainment and Driver Assistance (IDA) Business Line, Automotive Business Unit, working as Radar Product Architect. Early In his career he became a specialist in RF frequency synthesizers and contributed to many RF products that became market leaders in their segments, such as TV tuners, car-radio ICs, and integrated L-band receivers for satellite set-top boxes. He then led the project team that developed and industrialized the first silicon-based receiver IC for 12 GHz satellite outdoor units. Steadily moving towards higher frequencies, from 2008 till 2011 he coordinated the European industrial and academic consortium "Qstream", consisting of 20 partners, towards a realization of 40nm-CMOS high-bit-rate wireless data communication systems operating in the 60 GHz frequency band. From 2012 to present, Cicero led the NXP transition from mmWave communication systems into advanced automotive radar applications in the 76-81 GHz frequency band and is presently working on the industrialization of the first single-chip radar transceiver in 40nm CMOS technology. His research activities and interests include microwave and mm-Wave transceiver architectures, radar system implementation and signal processing, and implementation of circuit building blocks. He is the author of Architectures for RF Frequency Synthesizers (Boston, MA: Kluwer, 2002) and is a co-author of Circuit Design for RF Transceivers (Boston, MA: Kluwer, 2001). He is a (co-) inventor of 28 unique patent families, filed in the US, Europe, and far-eastern countries. Presently, he is acting on the IEEE-MTT Wireless-Enabled Automotive and Vehicular Applications Technical Committee 27. He is a Senior Member of the IEEE, acting regularly as a reviewer for the SSC and MTT-S societies.